NANO LETTERS

Letter

pubs.acs.org/NanoLett

Single Molecule Conductance, Thermopower, and Transition Voltage

Shaoyin Guo,[†] Gang Zhou,[‡] and Nongjian Tao*,[†]

[†]Center for Bioelectronics and Biosensors, Biodesign Institute, and Department of Electrical Engineering, Arizona State University, Tempe, Arizona 85287, United States

[‡]Laboratory of Advanced Materials, Fudan University, Shanghai 200438, China

Supporting Information

ABSTRACT: We have measured the thermopower as well as other important charge transport quantities, including conductance, current–voltage characteristics, and transition voltage of single molecules. The thermopower has little correlation with the conductance, but it decreases with the transition voltage, which is consistent with a theory based on Landauer's formula. Since the transition voltage reflects the molecular energy level alignment, our finding also shows that the thermopower provides valuable information about the relative alignment between the molecular energy levels and the electrodes' Fermi energy level.

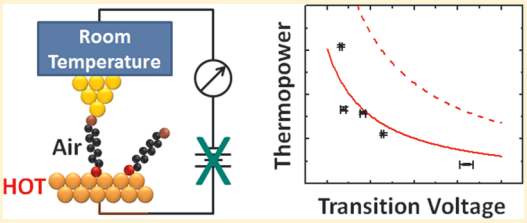

KEYWORDS: *Molecular electronics, single molecule thermopower, single molecule conductance, transition voltage spectroscopy, single molecule current–voltage characteristics, STM break junction*

Understanding charge transport through single molecules is the most fundamental goal in molecular electronics.[1−4] To achieve this goal, a variety of methods have been developed to measure the conductance, current–voltage characteristics, transition voltage spectroscopy (TVS), inelastic electron tunneling spectroscopy, and current-induced local heating of single molecules attached between two electrodes (molecular junctions).[5−16] In addition, the thermopower of molecular junctions have been measured by several groups recently[17−23] not only as an important parameter for characterizing molecular scaled thermal-electric energy conversion, but also as a useful method to provide new insights into the charge transport mechanism in molecules.

In the framework of Landauer's formula, the thermopower (or the Seebeck coefficient) of a metal–molecule–metal (MMM) junction is given by[24]

$$S_{\text{junction}} = -\frac{\pi^2 k_B{}^2 T}{3|e|}\frac{\partial \ln(\tau(E))}{\partial E}_{E=E_F} \quad (1)$$

where $\tau(E)$ is the transmission function of the junction. In other words, the thermopower is proportional to the slope of the transmission function (vs energy) at the Fermi level of the metal electrodes, which depends on the alignment between the electrode Fermi energy level and the molecular energy levels (e.g., highest occupied molecular orbital, HOMO, or lowest unoccupied molecular orbital, LUMO).[24] The energy level alignment is determined not only by the nature of the molecule and electrodes, but also by the interaction between the molecule and the electrodes. Determining the energy level alignment is critical for understanding the charge transport mechanism in single molecules, and the thermopower provides valuable information about the energy alignment. For example, if the slope is positive (negative S_{junction}), it means that the Fermi level is closer to the LUMO than to the HOMO, and consequently, the charge transport is dominated by electrons. On the other hand, if the slope is negative (positive S_{junction}), then the Fermi level is closer to the HOMO, and the charge transport is dominated by holes. In a simplified scenario where the HOMO and LUMO transmission peaks are described with by Lorentzian functions, more detailed molecular energy level alignment information can be obtained. This idea has been pursued by Baheti et al.[18] by combining thermopower measurements and model calculations, but the relationship between the energy level alignment and the thermopower has not been studied experimentally.

Here we report on the study of the thermopower, conductance, and current–voltage characteristics, as well as TVS of single molecule junctions. Because TVS is a measure, if not direct, of the energy alignment between the frontier molecular orbital and the Fermi level of the electrodes,[25−30] we determined the relationship between the energy level alignment and the thermopower by studying molecules with different transition voltages.

Experimental Section. The thermopower of molecular monolayers bridged between a scanning tunneling microscope (STM) tip and a gold substrate has been studied by directly measuring the voltage across molecules due to a temperature gradient applied between the tip and substrate.[17] More recently, the thermoelectric effect of single molecules has been studied by measuring zero-bias current induced by a temperature gradient between a STM tip and a substrate.[23] In this work, we measured the conductance, thermopower, $I-V$ characteristics,

Received: June 10, 2013
Revised: July 16, 2013

   dx.doi.org/10.1021/nl4021073 | *Nano Lett.* XXXX, XXX, XXX−XXX

and TVS using a similar temperature setup in STM (Figure 1): a gold substrate covered with target molecules was mounted

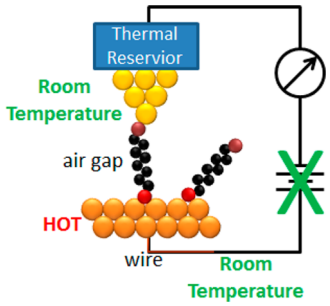

Figure 1. Schematic illustration of the experimental setup for studying the thermoelectric effect of single molecules.

onto a STM sample holder with a resistive heating plate and a thermocouple. The temperature was monitored and controlled by a LakeShore 331 temperature controller. Similar to the previous works,[17,23] the STM tip was in direct contact with an electrically shielded metal block, which acted as a thermal reservoir so that the STM tip temperature could be kept at room temperature. A gold wire was used to apply the bias to the heated substrate. A clean Teflon cell was used to hold clean toluene to protect the SAM surface during the preparation stage of the experiment. The toluene was then removed from the cell using a clean glass pipet before the STM setup was placed into a glovebox filled with nitrogen for thermoelectric measurement.

We then carried out the measurements using a STM break junction technique based on the following procedures:[13] (1) The STM tip was moved into the substrate until close enough to for the molecules to bridge the tip and the substrate but without forming the atomic contacts with the substrate. (2) The tip was pulled away from the substrate, during which the current was monitored continuously. When a step in the current was detected, signaling the formation of a molecular junction,[10] the tip was held in position and an current (I)−voltage (V) curve was recorded. (3) The tip was pulled away from the substrate by an additional distance. If the current did not drop abruptly, indicating that the molecular junction was still intact, another $I-V$ curve was recorded. Otherwise, the measurement started over again.

By repeating the procedures above, we acquired a large number of $I-V$ curves for a given temperature difference between the tip and substrate. The current and voltage interceptions of the $I-V$ curve are the thermoelectric current and voltage, respectively, and the slope determines the conductance of the single molecule junction. Because of the relatively small thermopower values, we swept the bias voltage over a small range (e.g., 5 mV) and measured the current with a relatively high gain current preamplifier (1 n A/V or 10 nA/V) in order to measure the voltage interception accurately and minimize zero bias current offset of the circuit (Supporting Information). For TVS measurement, however, we swept the voltage over a wider range (>1 V) and measured the current with a lower gain preamplifier (1 μA/V or 100 nA/V). A more detailed description of the experimental setup is given below.

The gold substrates used were prepared by thermally evaporating gold (thickness ∼ 130 nm) on freshly cleaved mica under UHV. Each substrate was then briefly annealed using a hydrogen flame and immersed into solutions containing a sample molecule (typically ∼50 μM concentration) for overnight. For short alkanedithiols (e.g., 1,4-butanedithiol) and conjugated molecules (e.g., 4,4′-dimercaptostilbene), the

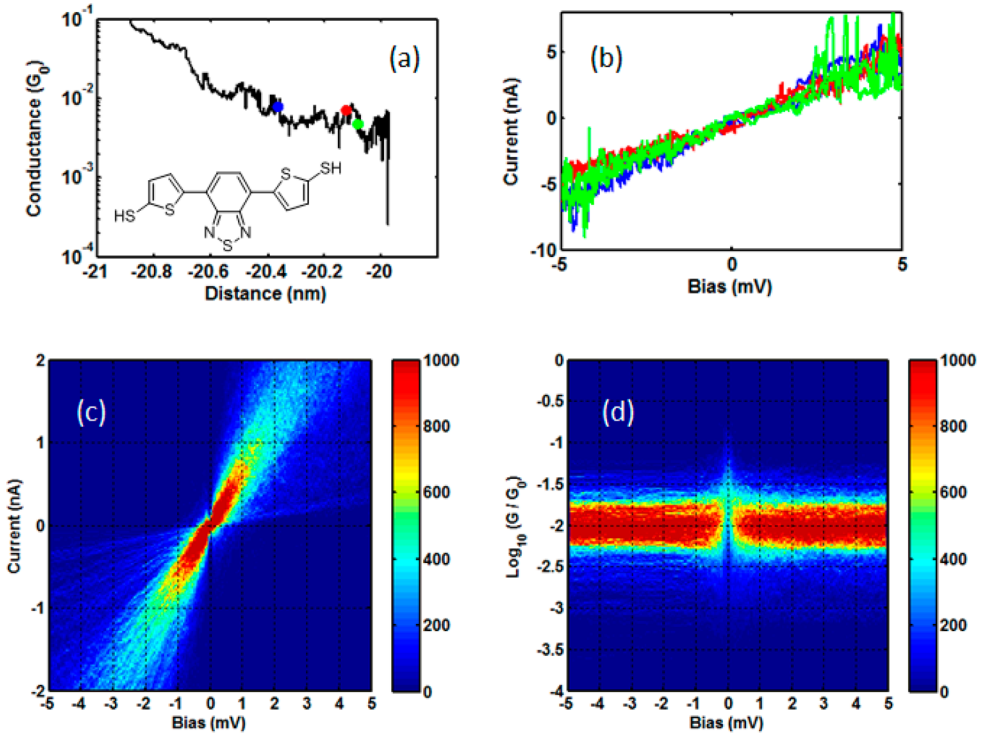

Figure 2. (a) A typical current−distance trace of DTBTDT. (b) $I-V$ curves measured at the positions marked by the colored dots shown in a. (c) A 2-D histogram of $I-V$ curves. (d) A 2-D histogram of conductance-bias ($G-V$) curves. Note: The conductance was obtained by dividing current by bias.

dx.doi.org/10.1021/nl4021073 | *Nano Lett.* XXXX, XXX, XXX−XXX

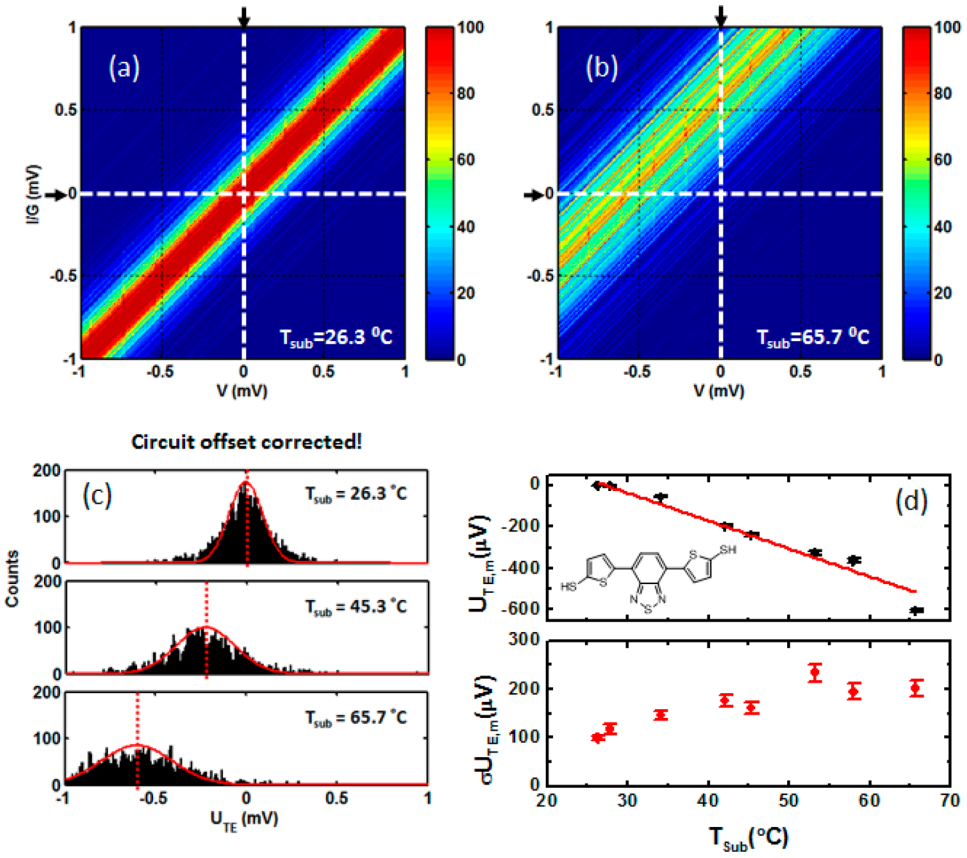

Figure 3. (a) A histogram of normalized $I-V$ curves for DTBTDT with no temperature difference between the STM tip and substrate. (b) A histogram of normalized $I-V$ curves with a finite temperature difference between the STM tip and substrate, from which the thermoelectric voltages across single DTBTDT junctions were extracted from zero bias current or zero current bias (white dashed lines). (c) 1-D thermoelectric voltage histograms extracted at different substrate temperatures (temperature differences). (d) Average thermoelectric voltages (top panel) and corresponding distributions (bottom panel) plotted against substrate temperatures. The red straight line is a linear fit to the average thermoelectric voltage versus temperature difference plot. From the slope of the linear fit the thermopower of DTBTDT was obtained.

current tended to jump to saturation of the current amplifier or short circuit at high bias. The phenomenon has been reported previously and attributed to the migration of gold atoms under the large electric field.[31,32] To minimize this instability, the sample molecule was mixed with a monothiolated alkane molecule with a length similar to that of the sample molecule at a ratio of 1:3 (total concentration of ~50 μM). We found that the presence of monothiolated alkane molecules passivated the electrodes and greatly reduced the chance of short circuit at large bias voltages. To ensure that the monothiols did not introduce artifacts in the STM break junction measurement, control experiments using the substrate covered with each of the monothiols were carried out, and the current traces were found to be featureless, indicating that the monothiols did not form molecular junctions.

Results and Discussion. *Small-Bias I–V and G–V Statistics.* Figure 2a shows a typical current–distance trace of 4,7-dithiophenyl-2,1,3-benzothiadiazole-3′,3″-dithiol (DTBTDT), where the step indicates the formation of a single molecule junction. Along the current step, multiple $I-V$ curves were obtained until the current dropped abruptly, signaling the breakdown of the molecular junction. Plotted in Figure 2b are three representative $I-V$ curves recorded at points marked by colored dots on the current step shown in Figure 2a, where the color of each $I-V$ curve matches the color of the corresponding dot in Figure 2a. Within the small bias sweep range (±5 mV), the $I-V$ curves are linear as expected. A large number (typically over 1000) of such $I-V$ curves were obtained automatically at different substrate temperatures using an algorithm described previously[13] and used to construct 2-D $I-V$ histograms (Figure 2c). From the $I-V$ curves, $G-V$ ($G = I/V$) curves were also obtained with an example shown in Figure 2d. The $G-V$ histogram shows a flat band, which indicates good linearity of the $I-V$ curves at low bias voltages.

Thermoelectric Measurement. The thermopower of the molecular junction can be expressed by

$$S_{\text{junction}} = S_{\text{Au}} - \frac{\Delta U_{\text{TE,m}}}{\Delta T} = S_{\text{Au}} - \frac{-\Delta(I_{\text{TE,m}}/G_{\text{m}})}{\Delta T} \qquad (2)$$

where S_{Au} is the thermopower of gold (~2 μV/K),[33] ΔT is the temperature difference across the molecular junction, $U_{\text{TE,m}}$ and $I_{\text{TE,m}}$ are the open circuit (zero current) voltage and short circuit (zero bias) current, respectively, and G_{m} is the conductance of the molecular junction. Similar to the previous work by Reddy et al.,[17] we controlled the substrate temperature, T_{sub}, and allowed the tip temperature to equilibrate with the surrounding environment via the metal block described in the Experimental Section.

According to eq 2, the thermopower can be determined from either $U_{\text{TE,m}}$ or $I_{\text{TE,m}}$ and G_{m} from the $I-V$ curves at low bias voltages. We fit each low-bias $I-V$ curve with a linear equation to obtain G_{m} and constructed $I/G_{\text{m}}-V$ histograms at different substrate temperatures (Figure 3a,b). At room temperature, the

dx.doi.org/10.1021/nl4021073 | Nano Lett. XXXX, XXX, XXX–XXX

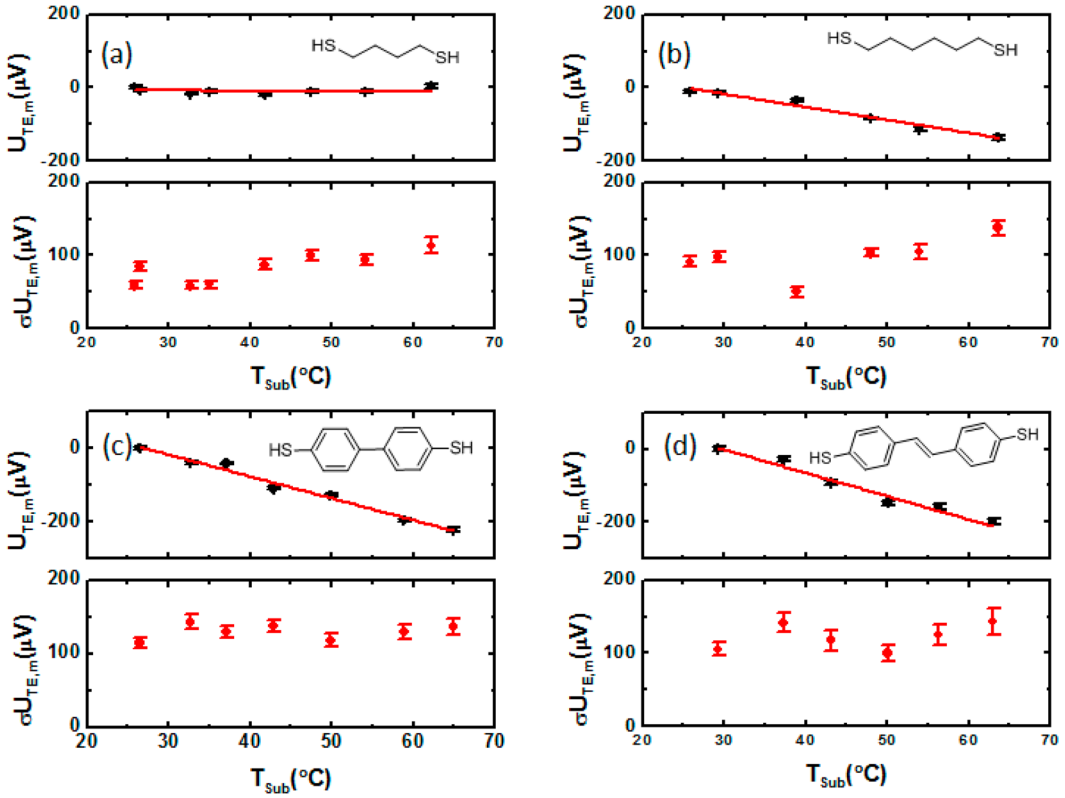

Figure 4. Thermoelectric voltages and corresponding distributions vs substrate temperature for (a) 1,4′-butanedithiol, (b) 1,6′-hexanedithiol, (c) 4,4′-biphenyldithiol, and (d) 4−4′-dimercaptostilbene single molecular junctions.

histogram shows a straight band with its center passing through the origin of the I/G_m-V histogram. Heating up the substrate, an offset voltage (current) appeared due to the thermoelectric effect, and consequently the center of the I/G_m-V histogram shifted away from the origin. One such example is shown in Figure 3b, from which $U_{TE,m}$ was extracted from the statistical average of the voltage (current) intersections.

It is important to note that in addition to the thermoelectric effect the circuit itself had also an intrinsic voltage or current offset, and the offset depended on the temperature at input lead (the STM tip). However, our tests showed that the metal block (thermal reservoir) attached to the STM tip helped stabilize the temperature of the tip and thus the voltage (current) offset of the circuit (Supporting Information). Because the intrinsic circuit offset was constant, we corrected it in the $I-V$ histograms in Figure 3a and b.

From the I/G_m-V histograms acquired at different substrate temperatures, we obtained thermoelectric voltage ($U_{TE,m}$) histograms by extracting the voltage interceptions. Figure 3c shows $U_{TE,m}$ histograms at different temperatures, revealing a systematic shift in the average of $U_{TE,m}$. The $U_{TE,m}$ histograms found here for single molecules are broader than the previously reported monolayer thermoelectric measurements,[17] but in agreement with the single molecule thermoelectric current measurement by Widawsky et al.[23] We will discuss the difference between single molecule and monolayer molecule measurements later.

Each histogram peak can be fit with a Gaussian distribution, where the peak position represents the average $U_{TE,m}$ (top panel of Figure 3d) and width of the Gaussian reflects the junction-to-junction variability (bottom panel of Figure 3d). Plotting the average of $U_{TE,m}$ versus temperature reveals a linear relationship between the $U_{TE,m}$ and temperature. To confirm the possibility that the temperature dependence of $U_{TE,m}$ was indeed due to the thermoelectric effect, rather than drift in the setup, we measured $U_{TE,m}$ by both ramping the temperature from low to high and from high to low values. Experimental data measured from both temperature ramping directions fall onto the same line, which verifies that the temperature dependence was originated from the thermoelectric effect. A linear fit of the plot gives rise to the thermopower of the molecular junction. For DTBTDT, we found that the thermopower is 15.46 ± 0.15 μV/K.

We carried out similar measurements on 1,4-butanedithiol (C4), 1,6-hexanedithiol (C6), 1,4′-biphenyldithiol (BPDT), and 4,4′-dimercaptostilbene (DMS). The average $U_{TE,m}$ and width of the $U_{TE,m}$ distribution vs T_{sub} for these molecules are plotted in Figure 4. The slopes of the plots determine the thermopower of the molecules.

Thermopower Variability. The thermopower of single molecules varies from junction to junction as shown by the distribution in the thermoelectric voltage histogram plotted in Figure 3c. A large junction-to-junction variability has been observed in the conductance of single molecules. In the case of tunneling-dominated electron transport, the conductance is described by $G = A\ \exp(-\beta L)$, where A is the contact conductance and β is the tunneling decay constant that depends on the alignment of the molecular energy levels relative to the electrode Fermi energy level. Our previous work[13] indicated that the large variability in the conductance is primarily due to the variability in the contact conductance (or resistance). The variability in the thermopower of single molecules could also be attributed the variability in the contact conductance. To examine this possibility, we plotted the 2-D

dx.doi.org/10.1021/nl4021073 | *Nano Lett.* XXXX, XXX, XXX−XXX

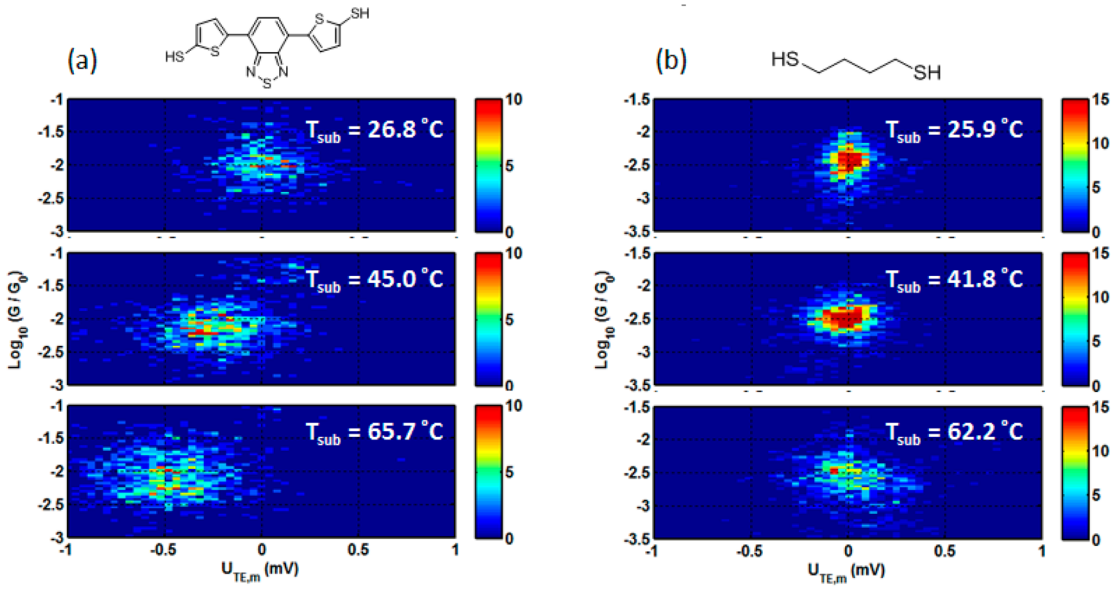

Figure 5. 2-D histograms of conductance vs thermoelectric voltage at different substrate temperatures for (a) DTBTDT and (b) C4.

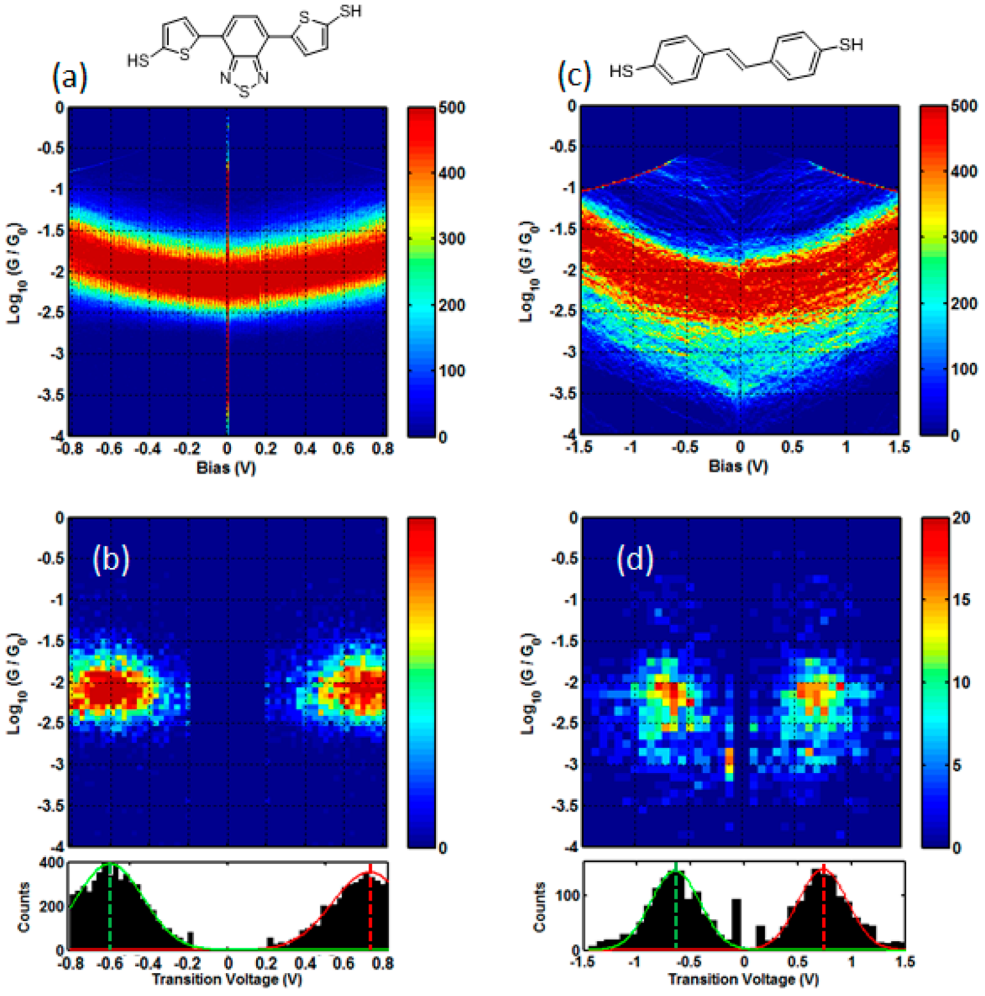

Figure 6. 2-D *G*−*V* histograms for DTBTDT (a) and (b) DMS. 2-D transition voltage histograms for DTBTDT (c) and DMS (d). 1-D transition voltage histograms are plotted at the bottom panels of c and d.

histograms of thermoelectric voltage and conductance at different substrate temperatures (Figure 5). From the histograms, we calculated the Pearson's correlation coefficients which determined that correlation between the thermopower and conductance was close to zero (typically smaller than 0.05), which indicates that the observed junction-to-junction thermo-

dx.doi.org/10.1021/nl4021073 | *Nano Lett.* XXXX, XXX, XXX−XXX

Table 1. Measured Thermopower, Transition Voltages, and Conductance[a]

molecule	thermopower (μV/K)	thermopower error (μV/K)	transition voltage (V)	transition voltage error (V)	conductance (G_0)
C4	2.11	0.11	2.1	0.075	4.5×10^{-3}
C6	5.55	0.13	1.14	0.015	6.2×10^{-4}
DTBTDT	15.46	0.15	0.66	0.011	9.2×10^{-3}
DMS	8.35	0.23	0.69	0.031	5.2×10^{-3}
BPDT	7.92	0.14	0.91	0.031	7.5×10^{-3}

[a]Note that the error is the fitting error of linear fitting for thermopower and that of Gaussian fitting for transition voltage. Conductance values are averages of all data sets at different substrate temperatures. No systematic temperature dependence was observed.

power variability was not directly related to the variability in the contact conductance.[13]

Another possible explanation of the thermopower variability is the variability in the alignment of the molecular energy levels relative to the electrode's Fermi energy level, according to the tunneling model by Paulsson et al.[24] as well as a recent theoretical work on thermopower of biphenyl based molecules.[34] This explanation also helps us to understand the relatively large thermopower distribution observed in the single molecule measurement compared to that in the monolayer measurement as we noted earlier.[17] In the case of single molecule measurement, the junction-to-junction variability in the energy level alignment is expected to be greater than the case of monolayer measurement, involving multiple molecules that average out fluctuations in the energy level alignment. An important quantity related to the energy level alignment is transition voltage of molecular junctions, which can be measured experimentally with TVS. We discuss below the correlation between transition voltage and thermopower.

Transition Voltage and Thermopower. As we have mentioned earlier, eq 1 indicates that the thermopower is related to the alignment of the molecular energy level relative to the electrodes' Fermi energy level. Bâldea[29,30] showed recently that, if one molecular energy level dominates the electron transport, and the molecule−electrode contact is symmetric and weak, then the thermopower is directly related to the transition voltage and given by Supporting Information

$$S_{\text{junction}} \approx -\frac{4\pi^2 k_B{}^2 T}{3\sqrt{3}\,e^2}\frac{1}{V_t} \approx \frac{A}{V_t} \qquad (3)$$

where V_t is the transition voltage and $A = 16.93$ μV·V/K.

To further study the relationship between thermopower and tunnel barrier height, we performed single molecule transition voltage spectroscopy using the procedure described previously.[13] Figure 6a and c shows the 2-D $G-V$ histograms for DTBTDT and DMS, where the bowl-shaped bands indicate the nonlinearity of the $I-V$ curves in high bias regimes. Figure 6b and d plots the transition voltage histograms for the two molecules, from which the average transition voltage and width of the distribution can be obtained. Table 1 summarizes thermopower and the corresponding transition voltages of each molecule.

Figure 7 plots the thermopower vs transition voltage for five different molecules. It shows that conjugated molecules typically have smaller transition voltages and larger thermopower, compared to the saturated alkanedithiols. This observation is consistent with the facts that conjugated molecules have lower tunnel barriers, or closer alignment between the HOMO energy level and the electrodes' Fermi energy levels. Figure 7 shows that the thermopower decreases with the transition voltage, as predicted by eq 3. The dashed

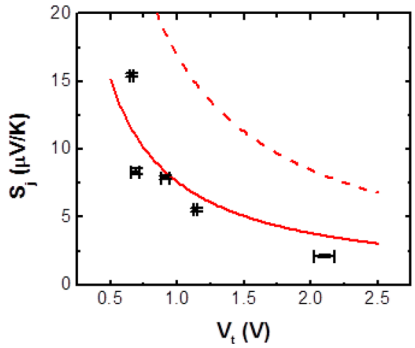

Figure 7. Measured thermopower plotted against measured transition voltage for different molecules.

red line in Figure 7 is the prediction of eq 3, $S_{\text{junction}} = 16.93/V_t$, which reproduces the trend of the thermopower but does not fit the experimental data. The best fit was obtained if $A = 7.6$ (solid red curve), about half of what the simple theory predicts. Given multiple simplifications in driving eq 3, this level of agreement between experimental data and theory is considered to be good. For example, the wide band assumption eliminates contribution of the other molecular orbitals (e.g., LUMO), which can reduce the measured thermopower values. In addition, Lorentzian distribution is a very coarse approximation to the transmission function profile while any subtle deviation can significantly alter the local slope at the Fermi level.

Conclusions. The single molecule conductance, $I-V$ characteristics, transition voltage, and thermopower were studied with a STM-break junction method for different molecules. For each molecule, a large amount of $I-V$ curves was recorded by varying the temperature difference between the STM tip and the substrate, from which both the conductance and thermoelectric voltage of a single molecule were determined simultaneously. The thermopower, or Seebeck coefficient, was extracted by linearly fitting the thermoelectric voltage vs substrate temperature. Single molecule transition voltage was also measured from the $I-V$ curves recorded over a wide bias voltage range. We found that the thermopower decreases with the transition voltage, which is consistent with the prediction of the tunneling-based theory within the framework of the Landauer formula. The study also shows that thermopower provides useful information molecular energy level alignment and contribute to the understanding of charge transport mechanism in single molecules.

■ ASSOCIATED CONTENT

Ⓢ Supporting Information

Experimental setup calibration, methods, and additional data. This material is available free of charge via the Internet at http://pubs.acs.org.

dx.doi.org/10.1021/nl4021073 | *Nano Lett.* XXXX, XXX, XXX−XXX

AUTHOR INFORMATION

Corresponding Author

*E-mail: njtao@asu.edu.

Notes

The authors declare no competing financial interest.

ACKNOWLEDGMENTS

The authors wish to thank NSF (CHE1105558) and ONR (N00014-11-1-0729) for financial support.

REFERENCES

(1) Song, H.; Reed, M. A.; Lee, T. *Adv. Mater.* **2001**, *23*, 1583−1608.
(2) Nitzan, A.; Ratner, M. A. *Science* **2003**, *300*, 1384−1389.
(3) Tao, N. J. *Nat. Nanotechnol.* **2006**, *1*, 173−181.
(4) McCreery, R. L. *Chem. Mater.* **2004**, *16*, 4477−4496.
(5) Huang, Z. F.; Xu, B. Q.; Chen, Y. C.; Di Ventra, M.; Tao, N. J. *Nano Lett.* **2006**, *6*, 1240−1244.
(6) Huang, Z. F.; Chen, F.; D'Agosta, R.; Bennett, P. A.; Di Ventra, M.; Tao, N. J. *Nat. Nanotechnol.* **2007**, *2*, 698−703.
(7) Smit, R. H. M.; Noat, Y.; Untiedt, C.; Lang, N. D.; van Hemert, M. C.; van Ruitenbeek, J. M. *Nature* **2002**, *419*, 906−909.
(8) Gonzalez, M. T.; Wu, S. M.; Huber, R.; van der Molen, S. J.; Schonenberger, C.; Calame, M. *Nano Lett.* **2006**, *6*, 2238−2242.
(9) Loertscher, E.; Weber, H. B.; Riel, H. *Phys. Rev. Lett.* **2007**, *98*, 176807.
(10) Xu, B. Q.; Tao, N. J. *Science* **2003**, *301*, 1221−1223.
(11) Haiss, W.; Van Zalinge, H.; Higgins, S. J.; Bethell, D.; Hoebenreich, H.; Schiffrin, D. J.; Nichols, R. J. *J. Am. Chem. Soc.* **2003**, *125*, 15294−15295.
(12) Jang, S. Y.; Reddy, P.; Majumdar, A.; Segalman, R. A. *Nano Lett.* **2006**, 2362−2367.
(13) Guo, S.; Hihath, J.; Díez-Pérez, I.; Tao, N. *J. Am. Chem. Soc.* **2011**, *133* (47), 19189−19197.
(14) Hihath, J.; Arroyo, C. R.; Rubio-Bollinger, G.; Tao, N. J.; Agrait, N. *Nano Lett.* **2008**, *8*, 1673−1678.
(15) Hihath, J.; Bruot, C.; Tao, N. *ACS Nano* **2010**, *4* (7), 3823−3830.
(16) Hihath, J.; Bruot, C.; Nakamura, H.; Asai, Y.; Díez-Pérez, I.; Lee, Y.; Yu, L.; Tao, N. *ACS Nano* **2011**, *5* (10), 8331−8339.
(17) Reddy, P.; Jang, S. Y.; Segalman, R. A.; Majumdar, A. *Science* **2007**, *315*, 1568−1571.
(18) Baheti, K.; Malen, J. A.; Doak, P.; Reddy, P.; Jang, S.-Y.; Tilley, T. D.; Majumdar, A.; Segalman, R. A. *Nano Lett.* **2008**, *8* (2), 715−719.
(19) Malen, J. A.; Doak, P.; Baheti, K.; Tilly, T. D.; Majumdar, A.; Segalman, R. A. *Nano Lett.* **2009**, *9*, 3406−3412.
(20) Malen, J. A.; Doak, P.; Baheti, K.; Tilley, T. D.; Segalman, R. A.; Majumdar, A. *Nano Lett.* **2009**, *9* (3), 1164−1169.
(21) Malen, J. A.; Yee, S. K.; Majumdar, A.; Segalman, R. A. *Chem. Phys. Lett.* **2010**, *491*, 109−122.
(22) Tan, A.; Balachandran, J.; Sadat, S.; Gavini, V.; Dunietz, B. D.; Jang, S.-Y.; Reddy, P. *J. Am. Chem. Soc.* **2011**, *133* (23), 8838−8841.
(23) Widawsky, J. R.; Darancet, P.; Neaton, J. B.; Venkataraman, L. *Nano Lett.* **2011**, *12* (1), 354−358.
(24) Paulsson, M.; Datta, S. *Phys. Rev. B* **2003**, *67* (24), 241403.
(25) Beebe, J. M.; Kim, B.; Gadzuk, J. W.; Frisbie, C. D.; Kushmerick, J. G. *Phys. Rev. Lett.* **2006**, *97* (2), 026801.
(26) Beebe, J. M.; Kim, B.; Frisbie, C. D.; Kushmerick, J. G. *ACS Nano* **2008**, *2*, 827−832.
(27) Huisman, E. H.; Guedon, C. M.; van Wees, B. J.; van der Molen, S. J. *Nano Lett.* **2009**, *9*, 3909−3913.
(28) Mirjani, F.; Thijssen, J. M.; van der Molen, S. J. *Phys. Rev. B* **2011**, *84* (11), 115402.
(29) Bâldea, I. *J. Am. Chem. Soc.* **2012**, *134* (18), 7958−7962.
(30) Bâldea, I. *Chem. Phys.* **2012**, *400*, 65−71.
(31) Gimzewski, J. K.; Möller, R. *Phys. Rev. B* **1987**, *36* (2), 1284−1287.
(32) Díez-Pérez, I.; Hihath, J.; Lee, Y.; Yu, L.; Adamska, L.; Kozhushner, M. A.; Oleynik, I. I.; Tao, N. *Nat. Chem.* **2009**, *1* (8), 635−641.
(33) Blatt, F. J.; Schroeder, P. A.; Foiles, C. L.; Greig, D. *Thermoelectric Power of Metals*; Plenum Press: New York, 1976; pp xv, 264.
(34) Bürkle, M.; Zotti, L. A.; Viljas, J. K.; Vonlanthen, D.; Mishchenko, A.; Wandlowski, T.; Mayor, M.; Schön, G.; Pauly, F. *Phys. Rev. B* **2012**, *86* (11), 115304.